Highly Sensitive Glucose Sensor Based on Pt Nanoparticle/Polyaniline Hydrogel Heterostructures

Dongyuan Zhai,[†,‡] Borui Liu,[†,§] Yi Shi,[‡] Lijia Pan,[‡,*] Yaqun Wang,[‡] Wenbo Li,[‡] Rong Zhang,[‡] and Guihua Yu[§,*]

[‡]School of Electronic Science and Engineering, National Laboratory of Microstructures (Nanjing), Nanjing University, Nanjing 210093, China and [§]Materials Science and Engineering Program and Department of Mechanical Engineering, The University of Texas at Austin, Austin, Texas 78712, United States. [†]These two authors contributed equally to this work.

ABSTRACT Glucose enzyme biosensors have been shown useful for a range of applications from medical diagnosis, bioprocess monitoring, to beverage industry and environmental monitoring. We present here a highly sensitive glucose enzyme sensor based on Pt nanoparticles (PtNPs)-polyaniline (PAni) hydrogel heterostructures. High-density PtNPs were homogeneously loaded onto the three-dimensional (3D) nanostructured matrix of the PAni hydrogel.

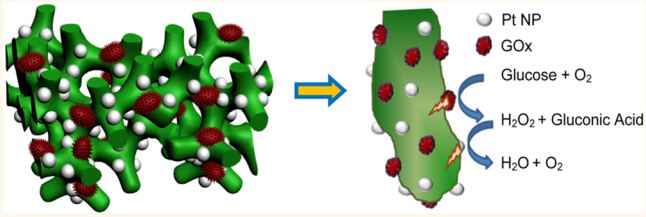

The PtNP/PAni hydrogel heterostructure-based glucose sensor synergizes the advantages of both the conducting hydrogel and the nanoparticle catalyst. The porous structure of the PAni hydrogel favored the high density immobilization of the enzyme and the penetration of water-soluble molecules, which helped efficiently catalyze the oxidation of glucose. In addition, the PtNPs catalyzed the decomposition of hydrogen peroxide that was generated during the enzymatic reaction. The transferred charges from these electrochemical processes were efficiently collected by the highly conducting PtNP/PAni hydrogel heterostructures. The glucose enzyme sensor based on this heterostructure exhibited unprecedented sensitivity, as high as 96.1 $\mu A \cdot mM^{-1} \cdot cm^{-2}$, with a response time as fast as 3 s, a linear range of 0.01 to 8 mM, and a low detection limit of 0.7 μM.

KEYWORDS: glucose sensors · polyaniline · conductive hydrogel · nanostructures · biosensors

Since the initial development of glucose enzyme electrodes by Clark and Lyons in 1962, tremendous effort has been directed toward research into glucose enzyme biosensors because of their great promise in a vast range of application fields such as medical diagnosis, diabetes management, bioprocess monitoring, beverage industry, and environmental monitoring.[1−10] Recently, Heller and Inganäs proposed that redox hydrogels and conducting polymer hydrogels can combine the advantages of both soft materials and organic conductors to be excellent biosensor electrode materials.[11,12] There is the growing interest in conducting polymer hydrogels, which have shown numerous features for high performance biosensors. The potential advantages include the following: (1) the combination of salvation and diffusion enables the conducting hydrogel to be permeable to water-soluble biochemical and chemicals; (2) the good biocompatibility of hydrogels promotes the immobilization of biomolecules and preserves their bioactivity; (3) the excellent electronic properties of conducting polymers due to their long π-conjugated backbone facilitate the rapid electron transferring; (4) the three-dimensional (3D) continuous conducting matrix of the hydrogel favors efficient charge collection; and (5) the scalable synthesis and fabrication of the conducting polymer hydrogel enables low cost patterning technologies such as inkjet printing and spray coating.[11−13]

Currently improving the sensing performance of enzyme electrodes continues to be the main focus of biosensor research. For amperometric-type glucose sensors, glucose oxidase (GOx) is the most commonly used enzyme for the specific recognition of glucose. GOx converts glucose into gluconolactone following reduction of the flavine adenine dinucleotide (FAD) prosthetic group. The cofactor is then reoxidized during the second reaction, within which two electrons and two protons are transferred to molecular oxygen, yielding hydrogen

* Address corresondence to ljpan@nju.edu.cn, ghyu@austin.utexas.edu.

Received for review January 29, 2013 and accepted March 10, 2013.

Published online March 11, 2013
10.1021/nn400482d

peroxide. As a result, the concentration of glucose can be monitored by detecting the formation of hydrogen peroxide.[14,15] However, the conducting polymer itself does not have catalytic activity, which is necessary for the electrochemical oxidization of the H_2O_2 at the detection potential used in the glucose sensors, which has limited their performance of glucose sensors.[16] Therefore, developing the conducting matrix that combines GOx immobilization and the catalytic materials, such as PtNPs, for the electro-oxidation of hydrogen peroxide are necessary for constructing high-performance glucose sensors. Recently, noble metallic micro/nanoparticles loaded onto conducting polymers, carbon nanotubes, and graphene substrates have been reported as efficient routes for increasing the sensitivity, selectivity, and electrode life of glucose sensors.[10,16−18] However, there have yet been any reports about glucose sensors that combine the advantages of both conductive polymer hydrogels and noble metal nanoparticles.

Herein, we report an ultra-high-sensitivity glucose sensor based on the PtNP/PAni hydrogel heterostructured electrodes. The monodisperse PtNPs, which were densely loaded onto the hydrogel matrix, acted as highly active catalysts for the electro-oxidation of hydrogen peroxide. Additionally, the 3D-microstructured conducting polymer hydrogel played important roles in the dispersion of PtNPs and as the GOx immobilization matrix and provided an electronically continuous 3D path for efficient charge collection (Figure 1). The glucose enzyme sensor based on the PtNP/PAni hydrogel heterostructures exhibited unprecedented sensitivity, as high as 96.1 $\mu A \cdot mM^{-1} \cdot cm^{-2}$, with an average response time of 3 s, a linear range from 0.01 to 8 mM, and a low detection limit of 0.7 μM.

RESULTS AND DISCUSSION

Synthesis of PtNP/PAni Hydrogel Heterostructure and Structural Characterization. The PAni hydrogel was synthesized by mixing aqueous solution of aniline (the monomer) and phytic acid (the cross-linker) with another solution containing ammonium persulfate (the initiator). The mixed precursor solution's color changed to dark green, and the solution was gelated to form a hydrogel within 3 min. The gelation of the PAni hydrogel was resulted from the protonatation reaction between phytic acid and the nitrogen groups on PAni. Because each phytic acid molecule interacts with more than one PAni chain, this cross-linking effect forms a mesh-like 3D hydrophilic network that maintains a high water content resulting in the formation of the hydrogel.[13] The mixed precursor solution had good wettabillty on the platinum surface. Therefore, a very thin film of the PAni hydrogel could be coated homogeneously onto the platinum electrode. The as-prepared hydrogel electrode was then immersed in an aqueous solution of H_2PtCl_6. Next, formic acid was added to reduce the H_2PtCl_6, converting it to PtNPs that were anchored onto the PAni hydrogel matrix.

The images obtained from scanning electron microscopy (SEM) and transmission electron microscopy (TEM) clearly revealed the morphology of the PtNP/PAni heterostructure. The SEM images in Figure 2a,b indicated that the PtNP/PAni hydrogel had a porous 3D hierarchical microstructure, which consists of interconnected PAni nanofibers with diameters of approximately 100 nm. The magnified SEM image shown in Figure 2b revealed that the PtNPs were evenly dispersed onto the 3D matrix of PAni. Further investigation by TEM confirmed that the Pt nanoparticles were homogeneously and densely coated onto the PAni nanofibers, as shown as Figure 2c. The PtNPs had monodispersed diameters of approximately 2 nm, which was determined by the statistical size distribution of the PtNPs shown in the inset of Figure 2c. Figure 2d shows the HRTEM lattice image of the PtNPs. The lattice spacing of 0.23 nm, marked in Figure 2d, is consistent with that of Pt (111) planes, and the lattice spacing of 0.20 nm could be attributed to the Pt (100) planes.[17,19] All these results indicated that the PAni hydrogel played an important role as a matrix for the homogeneous high-density loading and monodiameter dispersion of the PtNPs. The small size, monodispersed diameters, and homogeneous loading of the PtNPs are important parameters for promoting the performance of our glucose sensors.

The open channel of the 3D PAni hydrogel matrix provided an enlarged specific surfaces for enzyme

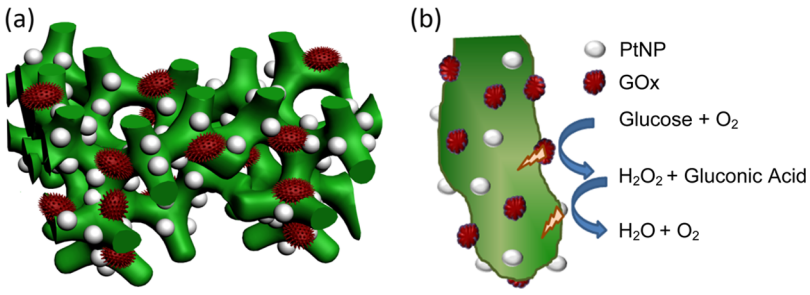

Figure 1. (a) Schematic representation of the 3D heterostructure of the PtNP/PAni hydrogel, in which the PAni hydrogel acts as a matrix for the immobilization of the GOx enzyme and homogeneous loading of PtNPs. (b) A 2D scheme showing the reaction mechanism of the glucose sensor based on the PtNP/PAni hydrogel heterostructure.

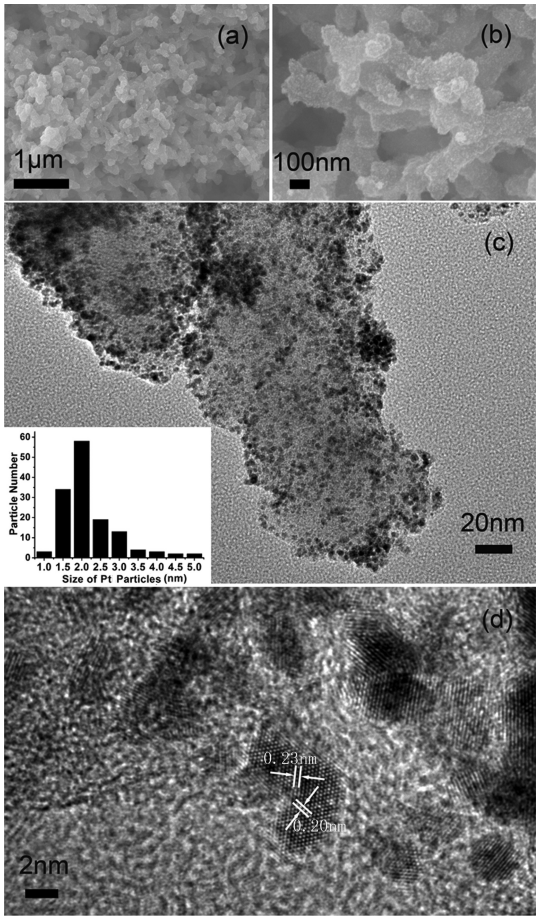

Figure 2. Morphologies of the PtNP/PAni hydrogel heterostructures. (a) SEM image showing the 3D hierarchical microstructure of the PtNP/PAni hydrogel. (b) Magnified SEM image of the homogeneous loading of PtNPs on the surface of the PAni hydrogel. (c) TEM image indicating the high density of the PtNPs loaded onto the PAni hydrogel matrix. Inset shows the statistical distribution of the PtNP sizes. (d) HR-TEM image of the PtNPs on the PAni hydrogel.

immobilization and facilitate the transport of molecules and electrons. The porous nanoscale framework offered a greater effective surface area than the bulk materials, which is essential for increasing the quantity of immobilized enzyme and enhancing the sensitivity of glucose sensors.[20] It should be noted that the dried PtNP/PAni hydrogel absorbed the enzyme solution and swelled back to its original volume quickly owing to the hydrophilic nature of the phytic acid-doped PAni. The number of phosphorus groups was excessive compared to that of the amine groups of PAni in our formula, which served to render the PAni hydrophilic. The PAni hydrogel had a water content as high as 93%. In addition, the porous nanostructure was beneficial for the diffusion of glucose molecules to the immobilized enzyme or H_2O_2 molecules to the anchored PtNPs, which resulted in the fast response of our glucose sensors to the analyzed substances.

The chemical structure of the PtNP/PAni hydrogel was characterized by Fourier transform infrared spectroscopy (FTIR) and X-ray photoelectron spectroscopy (XPS). As shown in the FTIR spectrum in Figure S1, the chemical structure of PAni was identical to that of an acid doped emeraldine PAni salt, with two characteristic peaks located at 1580 and 1491 cm^{-1} that corresponded to the stretching vibrations of the quinoid and benzenoid rings, respectively.[21,22] We chose the formic acid as the reductant to H_2PtCl_6, and it did not appear to affect the oxidation state of PAni. The state of PAni in the composite hydrogel was emeraldine rather than solely leucoemeraldine or permigraniline, which was important for maintaining the high conductivity of the PAni and the excellent sensitivity of glucose sensors. The absorption peak near 1143 cm^{-1} resulted from the N═Q═N (Q denotes quinoid ring) stretching mode, which was also an indication of the electron dislocalization in PAni.[9]

TABLE 1. Element Concentration of the PtNP/PAni Hydrogel Sample by XPS Analysis

C1s	N1s	O1s	Cl2p	Pt4f
61.30	8.64	12.51	0.97	16.59

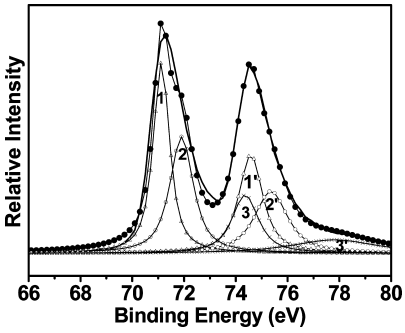

Figure 3. Pt 4f XPS spectrum of the PtNP/PAni hydrogel.

The XPS spectrum further confirmed the formation of the Pt metal in the hydrogel. Table 1 shows the elemental concentrations of the PtNP/PAni hydrogel. The atomic ratio of Pt/N was 1.92:1, indicating a high loading of PtNPs. Figure 3 shows the XPS spectrum of the Pt 4f core level region. The Pt $4f_{7/2}$ peak was deconvoluted into three groups of subpeaks labeled 1, 2, and 3, with binding energies of 71.1, 71.9, and 74.4 eV, respectively. The sub peak at 71.1 eV was assigned to Pt^0.[23] The second component that appeared at a higher binding energy of 71.9 eV was difficult to assign and may correspond to metallic Pt particles that were 1−2 nm or to Pt^{2+} (a byproduct of the reaction).[24] The sub peak at 74.4 eV was assigned to Pt^{4+}, indicating the formation of a trace amount of PtO_2.[25,26]

Performance of the Glucose Biosensor. Figure 4a shows a typical current−time response of the electrode at 0.56 V with successive addition of glucose. The current increased immediately with increases in the glucose concentrations, and it quickly reached a steady-state.

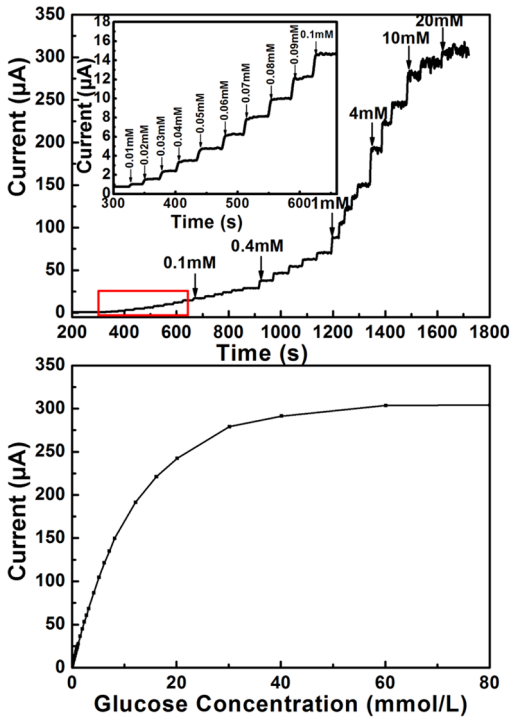

Figure 4. (a) Amperometric response of the PtNP/PAni hydrogel electrode after successive addition of glucose in 0.1 M PBS (pH = 5.6) at an applied potential of 0.56 V. Inset: the magnified part of the curve marked with red square. (b) The calibration curve for glucose concentrations from 1 μM to 80 mM.

The average response time of our sensor was as short as 3 s (reaching 95% of steady state current). Figure 4b shows the plot of the current as a function of glucose concentration. The steady-state current of the enzyme sensor was linearly related to the amount of glucose that was added to the buffer solution within the concentration range of 0.01−8 mM with a correlation coefficient of 0.993. The sensitivity calculated from the linear portion of the calibration was as high as 96.1 $\mu A \cdot mM^{-1} \cdot cm^{-2}$, which was higher than previously reported values for sensor electrodes based on composite of Pt and PAni, polypyrrole, or multiwalled carbon nanotubes (MWCNT) listed in Table 2. Compared with these materials, the performance of the Pt/PAni hydrogel glucose sensor was superior because of its fast response time and high sensitivity. Note that the glucose sensor presented excellent linear current−concentration relationship at the low concentration regime ranging from 0.01 to 1 mM (Figure S2b). The linear coefficient was calculated to be 0.999 in this regime. To verify the sensing performance of the sensor, a blind test was carried out that the signal of particular concentration of glucose solution that was added suddenly was compared with the calibration curve. The concentration of the blind sample can be accurately measured as shown in Figure S5. Moreover, the fast response of our sensor was attributed to the 3D porous nanostructures that facilitated the diffusion of the glucose and the H_2O_2. The high sensitivity resulted from the 3D porous hydrogel matrix, which allowed for the immobilization of the enzyme and preserved the high activity of the enzyme and the catalytic effects of the PtNPs for the oxidation of the H_2O_2. The apparent Michaelis−Menten constant (K_m) was calculated according to the Lineweaver−Burk equation and was estimated to be 0.572.[27] This value was much lower than those previously reported for PAni glucose sensors, confirming the high sensitivity of our device.[28,29] As shown in Figure S2, the device offered a low detection limit of 0.7 μM at a signal-to-noise ratio of 3, which was superior to previously reported PAni glucose sensors.[30,31] The PtNP/PAni hydrogel glucose sensor also showed the selectivity to other electroactive molecule species. Under the concentration close to human physiological environment, our sensor showed almost no response to ascorbic acid (AA) or glutathione (GSH), and a negligible response to L-cysteine(Cys), as shown in Figure S3. To demonstrate that the glucose sensor was useful for continuously measuring the glucose concentration in solution, we performed the concentration-varying experiment in which concentration of glucose was increased first and the solution was diluted from higher to lower concentration. The device presented almost the same signals for the same glucose concentrations, indicating the potential for the glucose sensor to monitor glucose concentration continuously (Figure S6).

PtNPs played an important role as efficient catalysts that enhanced the performance of the PtNP/PAni hydrogel glucose sensor. Figure 5 shows the calibration plots for the increase in current as a function of H_2O_2 concentration for Pt electrode with PtNP/PAni hydrogel, and Pt electrode with PAni hydrogel only. The current increased as the concentration of H_2O_2 increase in each example. It should be noted that the PtNP/PAni hydrogel exhibited a significantly increased current response compared to the PAni hydrogel, indicative of the greatly improved catalytic activity due to the high loading of PtNPs. The H_2O_2 molecules had to overcome a long diffusion distance in the noncatalytic PAni hydrogel at a potential of 0.56 V to penetrate to the Pt plane electrode for current generation when H_2O_2 was produced near the GOx. No contribution to the current response was observed when H_2O_2 diffused in the opposite direction in the glucose solution. The diffusion distance of the H_2O_2 molecules was greatly reduced when the high-density PtNPs were homogeneously dispersed onto the surface of the 3D PAni hydrogel. Additionally, the PtNPs catalyzed the oxidization of the nearby H_2O_2 molecules and transferred the charges to the highly conducting PAni matrix (Figure 1). Therefore, the PtNP/PAni hydrogel heterostructure increased the current output and the sensitivity of the glucose sensor.

TABLE 2. Comparison of Analytical Performance of Glucose Sensors

electrodes	sensitivity (mA cm^{-2} M^{-1})	response time (s)	linear range (mM)	detection limit (μM)	K_m (mM)	ref
GOx/PPy/Pt/Al_2O_3	7.4	<4	0.5−10	30	7.01	32
GOx/MWCNT/Pt	52.7		0−28	30		33
Nafion/GOx/Cu_2S-MWCNT/GC	1.0		0.01−1	10		34
GOx/(Pt/C)/GC	125	<5	0−45	<300		35
GOx/Pt-DENs/PANI/CNT/Pt	42	5	0.001−12	0.5		30
GOx/Pt/MWNT-PANI/GCE	128		0.003−8.2	1	0.64	28
GOx/PAni/PAN/Pt	67.1		0.002−12	2	13	8
GOx/AuNPs/PAni/GC	73.25		0.001−0.8	0.5		10
Pt-DENs/GOx/Pt-DENs/PAni/PSS/GC	39.63	5	0.01−4.5	0.5		36
GOx/PtNP/PAni/Pt	96.1	3	0.01−8	0.7	2.35	this work

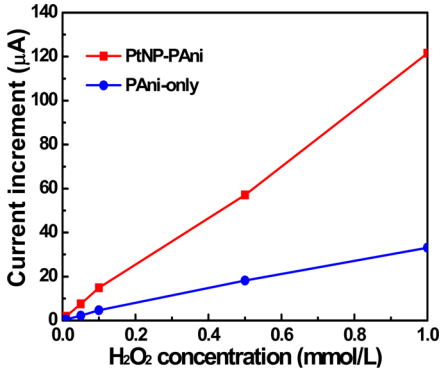

Figure 5. Calibration plots of the increase in current as a function of the H_2O_2 concentration of Pt electrode with PtNP/PAni hydrogel and Pt electrode with the PAni hydrogel.

By using the Pt-embedded PAni hydrogel, the Pt electrode was no longer the necessary substrate for glucose sensor. The Pt/PAni hydrogel sensor showed excellent performance with inexpensive glassy carbon (GC) electrode even without using the supporting Pt electrode, as shown in Figure S4. The electrocatalytic activity of Pt/PAni hydrogel sensor to oxidize H_2O_2 was increased up to 3 orders of magnitude as compared with the GC+PAni electrode (Figure S4a). The Pt/PAni hydrogel sensor also showed high sensitivity and wide-linear range of sensing to glucose (Figures S4a,b), which was in sharp contrast to the PAni hydrogel/GC electrode that almost had no response to the increase of glucose concentration. We envision that the material cost (amount of Pt used) in future commercialization could be greatly reduced by using the Pt/PAni hydrogel and other inexpensive substrates such as carbon/metal sheet/wire.

CONCLUSIONS

A glucose sensor with ultrahigh sensitivity and a rapid response time was constructed using a PtNP/PAni hydrogel heterostructure. The device combined the advantages of the 3D porous nanostructures of the PAni hydrogel and the PtNP catalyst. By efficiently reducing the diffusion length of the molecules and improving the charge transfer, the glucose sensors composed of the PtNP/PAni hydrogel heterostructure exhibited unprecedented performance with ultrahigh sensitivity, fast response, and a very low detection limit. We believe that this type of high-performance, hydrogel-based heterostructure glucose sensors, combined with a low-cost, scalable, microfabrication technique (such as inkjet or screen printing) shows great potential for use in applications relating to medical diagnosis, diabetes management, bioprocess monitoring, the beverage industry, and environmental monitoring.

MATERIALS AND METHODS

Preparation of the PtNP/PAni Hydrogel-Coated Electrodes. Aniline (ACS reagent, ≥99.5%), ammonium persulfate (ACS reagent, ≥98.0%), chloroform, and phytic acid (50%, w/w in water) were purchased from Sigma-Aldrich (St. Louis, Missouri, U.S.A.). The aniline monomer was distilled prior to use under reduced pressure. Phosphate-buffered saline (PBS) was also purchased from Sigma-Aldrich (St. Louis, Missouri, U.S.A.).

The PAni hydrogel was synthesized according to a previously published protocol.[13] Specifically, the hydrogel was synthesized by mixing two solutions labeled A and B. Solution A was prepared by dissolving 0.921 mL phytic acid in 2 mL of deionized (DI) water while stirring. Next, 0.458 mL of the aniline monomer (distilled prior to use) was added to the solution. Then, the solution was sonicated to form a clear solution. Solution B was prepared by dissolving 0.286 g ammonium persulfate in 1 mL of DI water. The color of the mixed solution containing A and B changed to dark green and formed a hydrogel within 3 min.

A total of 5 μL of the mixed solution containing A and B was coated onto a platinum electrode (diameter 5 mm, area ~0.1963 cm^2). Then, the electrode was transferred to a refrigerator (2 °C) and allowed to react for 10 min to form a thin homogeneous PAni hydrogel film on the surface of the Pt electrode. The electrode was immersed in DI water at a constant temperature of 40 °C for 30 min for purification and to remove any oligomers and excess ions.

The PAni hydrogel-modified Pt electrode was immersed into a solution containing 4.5 mL of deionized water, 9.65 μL of 1 mM H_2PtCl_6, and 0.25 mL of formic acid and allowed to react at room temperature for 12 h. Then, the electrode was washed several times with DI water to remove the excess ions and dried at 45 °C.

Immobilization of GOx on the PtNP/PAni Hydrogel Electrode. Glucose oxidase (glucose oxidase type II, ≥15000 units/g solid, Sigma)

was dissolved (40 mg/mL) in a 0.02 M PBS solution. Then, 10 μL of the GOx solution was deposited onto the electrode. The electrode was maintained under ambient conditions until it was dry. A total of 10 μL of 0.1% glutaraldehyde was added to the electrode and allowed to react for 4 h to cross-link the GOx with the PtNP/PAni hydrogel matrix. Finally, the prepared bioelectrode was washed thoroughly with 0.02 M PBS before storing it in 0.02 M PBS. The PAni was rehydrated to form a hydrogel after these processes.

Structural Characterization. The morphologies of the products were examined using a field emission SEM (LEO 1530), TEM JEM-40001X, and JEOL-2010 HR-TEM. FTIR spectra were recorded on a NEXUS 870 spectrophotometer. XPS measurements were performed on a VG-310F instrument using Al nonmonochromated X-rays (20 kV, 15 mA) with a hemispherical energy analyzer that was set to a pass energy of 100 eV for the survey spectrum and 20 eV for the peak scans. All of the spectra were charge shift corrected, with reference to the C 1s peak at 285.0 eV.

Electrochemical Characterization. The electrochemical experiments were performed with a CHI 660C electrochemical workstation (CH Instruments). A three-electrode cell with a sample volume of 50 mL was employed. The platinum electrode and a saturated calomel electrode (SCE) were employed as the counter electrode and the reference electrode, respectively. Amperometric detection was performed under an applied potential of −0.56 V. The solution was maintained at 35 °C and continuously stirred during the measurement with a magnetic stirring bar at a speed of 1030 rpm.

Conflict of Interest: The authors declare no competing financial interest.

Acknowledgment. L.P. and Y.S. are thankful for funding support from the Chinese National Key Fundamental Research Project (2013CB932900, 2011CB922100), the National Natural Science Foundation of China (61076017, 61229401, and 60990314), the Fundamental Research Funds for the Central Universities, and the Priority Academic Program Development of Jiangsu Higher Education Institutions (PAPD). G.Y. acknowledges the start-up funding provided by the Cockrell School of Engineering at the University of Texas at Austin.

Supporting Information Available: Additional experimental results, including FTIR spectrum and details of electrochemical testing and other control experiments. This material is available free of charge *via* the Internet at http://pubs.acs.org.

REFERENCES AND NOTES

1. Wang, J. Electrochemical Glucose Biosensors. *Chem. Rev.* **2008**, *108*, 814–825.
2. Newman, J. D.; Turner, A. P. F. Home Blood Glucose Biosensors: A Commercial Perspective. *Biosens. Bioelectron.* **2005**, *20*, 2435–2453.
3. Heller, A.; Feldman, B. Electrochemical Glucose Sensors and Their Applications in Diabetes Management. *Chem. Rev.* **2008**, *108*, 2482–2505.
4. Heller, A.; Feldman, B. Electrochemistry in Diabetes Management. *Acc. Chem. Res.* **2010**, *43*, 963–973.
5. Gerard, M.; Chaubey, A.; Malhotra, B. D. Application of Conducting Polymers to Biosensors. *Biosens. Bioelectron.* **2002**, *17*, 345–359.
6. Dhand, C.; Das, M.; Datta, M.; Malhotra, B. D. Recent Advances in Polyaniline Based Biosensors. *Biosens. Bioelectron.* **2011**, *26*, 2811–2821.
7. Gopalan, A. I.; Lee, K. P.; Ragupathy, D.; Lee, S. H.; Lee, J. W. An Electrochemical Glucose Biosensor Exploiting A Polyaniline Grafted Multiwalled Carbon Nanotube/Perfluorosulfonate Ionomer-Silica Nanocomposite. *Biomaterials* **2009**, *30*, 5999–6005.
8. Xue, H. G.; Shen, Z. Q.; Li, C. M. Improved Selectivity and Stability of Glucose Biosensor Based on *in situ* Electropolymerized Polyaniline−Polyacrylonitrile Composite Film. *Biosens. Bioelectron.* **2005**, *20*, 2330–2334.
9. Kausaite-Minkstimiene, A.; Mazeiko, V.; Ramanaviciene, A.; Ramanavicius, A. Enzymatically Synthesized Polyaniline Layer for Extension of Linear Detection Region of Amperometric Glucose Biosensor. *Biosens. Bioelectron.* **2010**, *26*, 790–797.
10. Xian, Y. Z.; Hu, Y.; Liu, F.; Xian, Y.; Wang, H. T.; Jin, L. T. Glucose Biosensor Based on Au Nanoparticles-Conductive Polyaniline Nanocomposite. *Biosens. Bioelectron.* **2006**, *21*, 1996–2000.
11. Heller, A. Electron-Conducting Redox Hydrogels: Design, Characteristics and Synthesis. *Curr. Opin. Chem. Biol.* **2006**, *10*, 664–672.
12. Asberg, P.; Inganas, O. Hydrogels of A Conducting Conjugated Polymer as 3-D Enzyme Electrode. *Biosens. Bioelectron.* **2003**, *19*, 199–207.
13. Pan, L. J.; Yu, G.; Zhai, D.; Lee, H. R.; Zhao, W.; Liu, N.; Wang, H.; Tee, B. C. K.; Shi, Y.; Cui, Y.; et al. Hierarchical Nanostructured Conducting Polymer Hydrogel with High Electrochemical Activity. *Proc. Natl. Acad. Sci. U.S.A.* **2012**, *109*, 9287–9292.
14. Li, Z. F.; Kang, E. T.; Neoh, K. G.; Tan, K. L. Covalent Immobilization of Glucose Oxidase on the Surface of Polyaniline Films Graft Copolymerized with Acrylic Acid. *Biomaterials* **1998**, *19*, 45–53.
15. Kim, H.; Lee, I.; Kwon, Y.; Kim, B. C.; Ha, S.; Lee, J.-h.; Kim, J. Immobilization of Glucose Oxidase into Polyaniline Nanofiber Matrix for Biofuel Cell Applications. *Biosens. Bioelectron.* **2011**, *26*, 3908–3913.
16. Zhou, H. H.; Chen, H.; Luo, S. L.; Chen, J. H.; Wei, W. Z.; Kuang, Y. F. Glucose Biosensor Based on Platinum Microparticles Dispersed in Nano-Fibrous Polyaniline. *Biosens. Bioelectron.* **2005**, *20*, 1305–1311.
17. Wu, J.; Yin, L. Platinum Nanoparticle Modified Polyaniline-Functionalized Boron Nitride Nanotubes for Amperometric Glucose Enzyme Biosensor. *ACS Appl. Mater. Inter.* **2011**, *3*, 4354–4362.
18. Guo, S.; Dong, S.; Wang, E. Polyaniline/Pt Hybrid Nanofibers: High-Efficiency Nanoelectrocatalysts for Electrochemical Devices. *Small* **2009**, *5*, 1869–1876.
19. Wang, J. S.; Li, J. J.; Yang, C. C. *In Situ* Preparation and the Characterization of Pt/SnO_2. *Chin. Chem. Lett.* **2012**, *23*, 371–374.
20. Gangadharan, R.; Anandan, V.; Zhang, A.; Drwiega, J. C.; Zhang, G. G. Enhancing the performance of a fluidic glucose biosensor with 3D electrodes. *Sens. Actuators, B* **2011**, *160*, 991–998.
21. Cao, Y.; Li, S. Z.; Xue, Z. J.; Guo, D. Spectroscopic and Electrical Characterization of Some Aniline Oligomers and Polyaniline. *Synth. Met.* **1986**, *16*, 305–315.
22. Tang, J. S.; Jing, X. B.; Wang, B. C.; Wang, F. S. Infrared-Spectra of Soluble Polyaniline. *Synth. Met.* **1988**, *24*, 231–238.
23. Jin, T.; Zhou, Y.; Mains, G. J.; White, J. M. Infrared and X-Ray Photoelectron-Spectroscopy Study of CO and CO_2 on Pt/CeO_2. *J. Phys. Chem.* **1987**, *91*, 5931–5937.
24. Eberhardt, W.; Fayet, P.; Cox, D. M.; Fu, Z.; Kaldor, A.; Sherwood, R.; Sondericker, D. Photoemission from Mass-Selected Monodispersed Pt Clusters. *Phys. Rev. Lett.* **1990**, *64*, 780–784.
25. Shyu, J. Z.; Otto, K. Characterization of Pt/Gamma-Alumina Catalysts Containing Ceria. *J. Catal.* **1989**, *115*, 16–23.
26. Daniel, D. W. Infrared Studies of CO and CO_2 Adsorption on Pt/CeO_2: the Characterization of Active-Sites. *J. Phys. Chem.* **1988**, *92*, 3891–3899.
27. Kamin, R. A.; Wilson, G. S. Rotating-Ring-Disk Enzyme Electrode for Biocatalysis Kinetic-Studies and Characterization of the Immobilized Enzyme Layer. *Anal. Chem.* **1980**, *52*, 1198–1205.
28. Zhong, H.; Yuan, R.; Chai, Y.; Li, W.; Zhong, X.; Zhang, Y. *In Situ* Chemo-Synthesized Multi-Wall Carbon Nanotube-Conductive Polyaniline Nanocomposites: Characterization and Application for A Glucose Amperometric Biosensor. *Talanta* **2011**, *85*, 104–111.
29. Matharu, Z.; Sumana, G.; Arya, S. K.; Singh, S. P.; Gupta, V.; Malhotra, B. D. Polyaniline Langmuir-Blodgett Film Based Cholesterol Biosensor. *Langmuir* **2007**, *23*, 13188–13192.
30. Xu, L.; Zhu, Y.; Yang, X.; Li, C. Amperometric Biosensor Based on Carbon Nanotubes Coated with Polyaniline/Dendrimer-Encapsulated Pt Nanoparticles for Glucose Detection. *Mater. Sci. Eng., C* **2009**, *29*, 1306–1310.

31. Horng, Y.-Y.; Hsu, Y.-K.; Ganguly, A.; Chen, C.-C.; Chen, L.-C.; Chen, K.-H. Direct-Growth of Polyaniline Nanowires for Enzyme-Immobilization and Glucose Detection. *Electrochem. Commun.* **2009**, *11*, 850–853.
32. Ekanayake, E. M. I. M.; Preethichandra, D. M. G.; Kaneto, K. Polypyrrole Nanotube Array Sensor for Enhanced Adsorption of Glucose Oxidase in Glucose Biosensors. *Biosens. Bioelectron.* **2007**, *23*, 107–113.
33. Xie, J.; Wang, S.; Aryasomayajula, L.; Varadan, V. K. Platinum Decorated Carbon Nanotubes for Highly Sensitive Amperometric Glucose Sensing. *Nanotechnology* **2007**, *18*.
34. Lee, H.; Yoon, S. W.; Kim, E. J.; Park, J. In Situ Growth of Copper Sulfide Nanocrystals on Multiwalled Carbon Nanotubes and Their Application as Novel Solar Cell and Amperometric Glucose Sensor Materials. *Nano Lett.* **2007**, *7*, 778–784.
35. Ammam, M.; Easton, E. B. High-Performance Glucose Sensor Based on Glucose Oxidase Encapsulated in New Synthesized Platinum Nanoparticles Supported on Carbon Vulcan/Nafion Composite Deposited on Glassy Carbon. *Sens. Actuators, B* **2011**, *155*, 340–346.
36. Xu, L.; Zhu, Y.; Tang, L.; Yang, X.; Li, C. Dendrimer-Encapsulated Pt Nanoparticles/Polyaniline Nanofibers for Glucose Detection. *J. Appl. Polym. Sci.* **2008**, *109*, 1802–1807.